Origin of perpendicular magnetic anisotropy of Ni-polyethylene coevaporated films

doi: 10.1063/1.354966

Origin of perpendicular magnetic anisotropy of Ni-polyethylene coevaporated films

Tsuyoshi Maro and Osamu Kitakami[a)]
Tsukuba Research Laboratory, Hitachi Maxell, Ltd., 6-20-1 Kinunodai, Yawara-mura, Tsukaba-gun, Ibaraki 300-24, Japan

(Received 23 November 1993; accepted for publication 24 August 1993)

The origin of the large perpendicular magnetic anisotropy ($0.5–1\times10^{-6}$ erg/cm^3) of Ni-polyethelene coevaporated films has been studied. It is indicated that the anisotropy can be very well explained by uniaxial anisotropy induced by the large tensile stress ($1–3\times10^{10}$ dyn/cm^2) through the inverse magnetostrictive effect. Other factors, such as magnetocrystalline or shape anisotropy, produce little effect on the perpendicular anisotropy of the films.

I. INTRODUCTION

Metal-polymer composite films exhibit unique physical properties. Their optical,[1,2] electrical,[3] and magnetic properties[4] have been extensively investigated. We have studied transition magnetic metal (TM) polyethylene (PE) coevaporated films (TM-PE films), and found that Fe (Ref. 5) and CoCr-PE[6] films become amorphous when the carbon content exceeds 9 at. % and the coercivity decreases to 1 Oe due to the disappearance of magnetocrystalline anisotropy. On the other hand, Ni-PE films[7] are in a polycrystalline state with the same carbon content, and have a large perpendicular magnetic anisotropy energy of 1×10^6 erg/cm^3. As the origin of the anisotropy in Ni-PE films has yet to be clarified, the temperature dependence of the magnetic properties, the crystallographic structures, and the internal stress were investigated.

In this article, we report the experimental results and discuss the origin of the perpendicular magnetic anisotropy.

II. EXPERIMENT

Ni-PE films were prepared by simultaneous coevaporation of Ni and PE (mean molecular weight 1000).[7] Two types of substrates were used: glass for measurements of magnetic properties, x-ray diffraction, and internal stress, and polyimide film for cross-sectional transmission electron microscopy (TEM) observation.

The vacuum chamber was evacuated to less than 1×10^{-6} Torr. The substrates were baked at 250 °C for 1 h and cooled to the preparation temperature. The Ni and PE were evaporated using, respectively, an electron gun and a resistance heating method. The carbon content in the Ni-PE films was varied by controlling the ratio of the deposition rate of the PE to that of the Ni. Details of the sample preparation conditions are shown in Table I.

The film thickness was measured using a surface roughness profilometer. The magnetic properties were measured using a vibrating sample magnetometer and a torque magnetometer in the temperature range of −195–425 °C. Samples were first cooled to −195 °C under no magnetic field. The magnetic properties were measured both in the heating process up to 425 °C and in the cooling process down to 50 °C. The temperature measurement was kept constant using a gas-flow-type temperature controller.

The internal stress in the films was determined from the curvature of the glass substrates which was measured by an optical lever method.

The crystallographic structures were studied by x-ray diffraction (line source: Cu$K\alpha$). The morphological structures were observed using a TEM. The carbon content in the films was determined by x-ray photoelectron spectroscopy.

III. RESULTS

The magnetic properties and carbon contents of the Ni-PE films are listed in Table II. The sign of the perpendicular magnetic anisotropy energy ($K_\perp$) without the demagnetization correction is defined to be positive when the axis of easy magnetization is in the normal direction of the film plane. The temperature dependence of the magnetic properties was measured for samples a–h and the internal stress for samples i–o. Samples a, b, i, j, and k contain 0.4–1.9 at. % carbon although they were prepared by evaporating only Ni. The reason for this is probably that PE molecules that had adhered to the inner wall of the vacuum chamber were released by the radiant heat from the molten Ni source during evaporation of the Ni, and were incorporated into the films.

A. Magnetic properties

Figure 1 shows the saturation magnetization (M_s) of the Ni-PE films at room temperature as a function of the

TABLE I. Preparation conditions for Ni-PE films.

Substrate temperature	50, 150 °C
Substrate	glass, polyimide film
Vacuum pressure	
background	$5–8\times10^{-7}$ Torr
during deposition	$1–2\times10^{-5}$ Torr
Deposition rate	
Ni	10–20 Å/s
polyethelyne	0–10 Å/s
Film thickness	4000–6000 Å

[a)]Present address: Research Institute for Scientific Measurements, Tohoku University, Katahira 2-1-1, Aoba-ku, Sendai, Miyagi 980, Japan.

 0021-8979/93/74(12)/7443/7/$6.00

TABLE II. List of substrate temperature T_s, film thickness δ, saturation magnetization M_s, perpendicular coercivity $H_{c_\perp}$, perpendicular magnetic anisotropy energy $K_\perp$ without the demagnetizing correction, and carbon content. The sign of $K_\perp$ is defined to be positive when the axis of easy magnetization is in the normal direction of the film plane.

Sample	T_s (°C)	δ (μm)	M_s (emu/cm^3)	$H_{c_\perp}$ (Oe)	$K_\perp$ (10^5 erg/cm^3)	Carbon content (at. %)
a	150	0.460	454.6	57.6	−7.500	1.4
b	50	0.429	446.4	64.0	−7.101	1.4
c	150	0.542	392.6	334.4	−1.185	3.9
d	50	0.499	386.2	284.2	−0.432	2.2
e	150	0.490	259.4	501.6	0.591	6.2
f	50	0.435	271.0	425.6	1.600	6.7
g	150	0.587	120.2	105.6	0.666	7.0
h	50	0.425	183.5	138.5	1.137	6.3
i	150	0.402	418.7	64.5	−6.987	1.0
j	50	0.450	460.4	82.5	−8.852	1.9
k	50	0.395	434.6	95.0	−8.565	0.4
l	150	0.456	339.9	381.0	−2.351	2.5
m	150	0.411	267.3	345.0	−0.957	4.5
n	150	0.316	197.8	206.0	−0.264	5.5
o	50	0.440	378.8	347.5	−1.061	2.7

carbon content. The M_s monotonically and rapidly decreases as the carbon content increases. The M_s of the Ni-PE films with 6–7 at. % carbon is less than half that of bulk Ni, suggesting that the Ni-PE films contain a large amount of a nonmagnetic or very weak ferromagnetic substance. Figure 2 shows the M_s dependence of the perpendicular coercivity ($H_{c_\perp}$) measured in the normal direction of the film plane. The $H_{c_\perp}$ reached a maximum at about 300 emu/cm^3. The $H_{c_\perp}$ of the Ni-PE films deposited at 150 °C is a little larger than that of those deposited at 50 °C.

The temperature dependencies of the M_s, $H_{c_\perp}$, and $K_\perp$ for samples a–h in Table II are shown in Figs. 3–5. The temperature dependence of the M_s for samples a and b in the heating and cooling processes is coincident with that of bulk Ni as measured by Weiss and Forrer.[8] The $H_{c_\perp}$ of

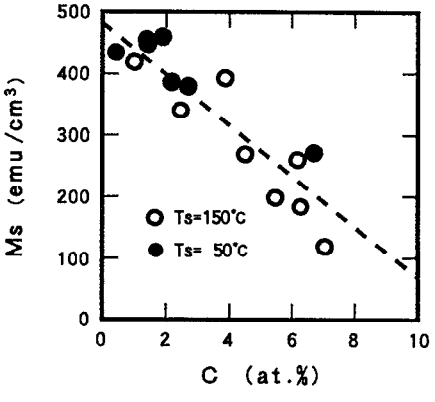

FIG. 1. Saturation magnetization (M_s) of the Ni-PE films at room temperature as a function of the carbon content. The open and closed circles indicate the M_s of the Ni-PE films deposited at the substrate temperatures of 150 and 50 °C, respectively.

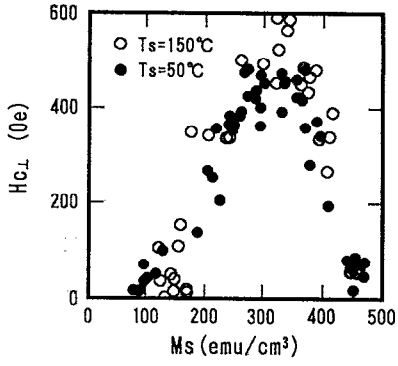

FIG. 2. Saturation magnetization M_s dependence of the coercivity $H_{c_\perp}$ of the Ni-PE films. The $H_{c_\perp}$ is the coercivity measured in the normal direction of the film plane. The open and closed circles indicate the $H_{c_\perp}$ of the Ni-PE films deposited at the substrate temperatures of 150 and 50 °C, respectively.

samples a and b is 40–60 Oe up to the Curie temperature of bulk Ni (358 °C) and is 0 Oe above this temperature. The temperature dependence of the $K_\perp$ of samples a and b shows a minimum around 100–200 °C.

In the case of the Ni-PE films (samples c–h), a large difference in the temperature dependence of the magnetic properties between the heating and cooling processes can be observed. The temperature dependence of the magnetic properties in the cooling process is in good agreement with that of samples a and b. The results indicate that irreversible changes occur in the magnetic properties by the heat treatment up to 425 °C. Since anomalous increases of the M_s and $H_{c_\perp}$ are observed at 150–250 °C in the heating

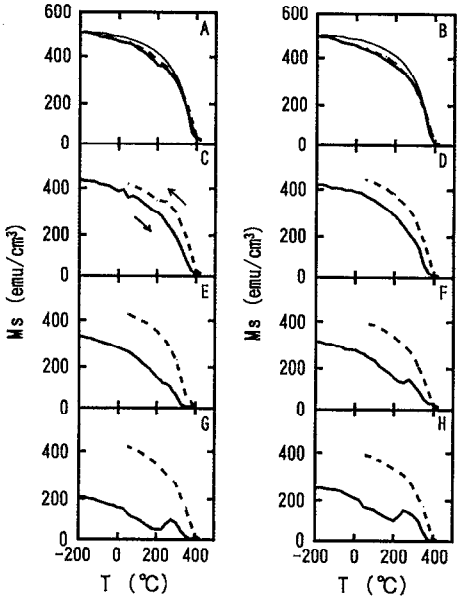

FIG. 3. Temperature dependence of the saturation magnetization M_s for samples a–h listed in Table II. The bold and dashed lines indicate the M_s curves in the heating and cooling processes, respectively. The fine lines shown in A and B provide the data on bulk Ni as measured by Weiss and Forrer (Ref. 8).

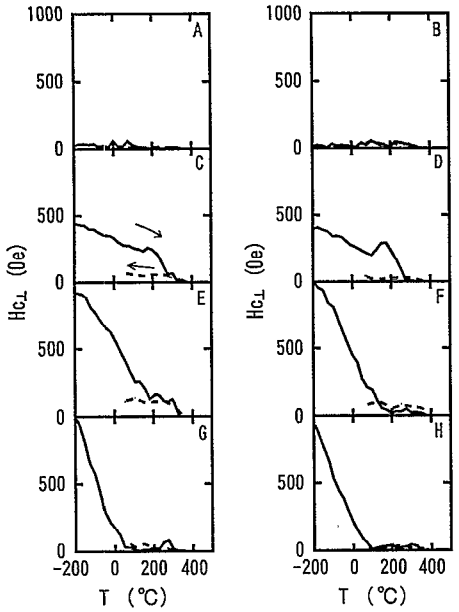

FIG. 4. Temperature dependence of the coercivity $H_{c_\perp}$ for samples a–h listed in Table II. The bold and dashed lines indicate the $H_{c_\perp}$ curves in the heating and cooling processes, respectively.

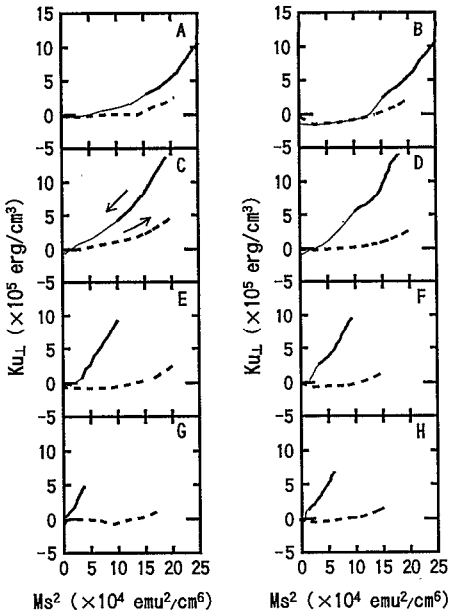

FIG. 6. Relation between the intrinsic perpendicular magnetic anisotropy energy ($K_{u_\perp}=K_\perp+2\pi M_s^2$) and M_s^2 for samples a–h. The solid and dashed lines indicate the relations in the heating and cooling processes, respectively. The bold part in the solid lines indicates data for the range of −190–150 °C.

process in Figs. 3 and 4, it can be supposed that the irreversible changes occur in this temperature region.

The relations between the intrinsic perpendicular anisotropy energy ($K_{u_\perp}=K_\perp+2\pi M_s^2$) and M_s^2 for samples a–h are shown in Fig. 6. The $K_{u_\perp}$ of the Ni-PE films in the heating process is nearly in proportion to the M_s^2 in the range of −195–150 °C (bold line in Fig. 6) as the carbon content increases. The results imply that the origin of the perpendicular magnetic anisotropy is due to shape anisotropy.

As mentioned above, the Ni-PE coevaporated films have higher perpendicular anisotropy than the Ni films when they incorporate several atomic percent of carbon from polyethylene. Such large perpendicular anisotropy diminishes with the heat treatment up to 425 °C.

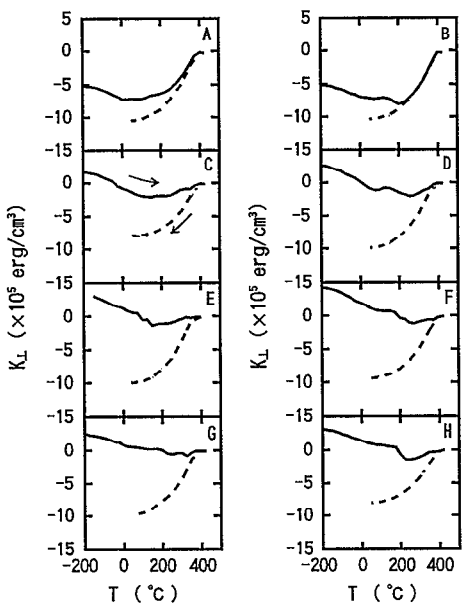

FIG. 5. Temperature dependence of the perpendicular magnetic anisotropy energy $K_\perp$ for samples a–h listed in Table II. The bold and dashed lines indicate the $K_\perp$ curves in the heating and cooling processes, respectively.

B. Structures of Ni-PE films

Figure 7 shows x-ray diffraction patterns of the Ni-PE film (sample h) before and after the heat treatment. All

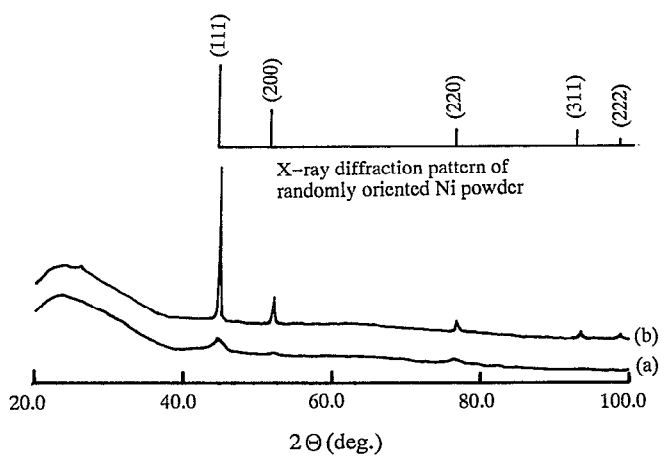

FIG. 7. X-ray diffraction patterns of the Ni-PE film (sample h) (a) before and (b) after the heat treatment.

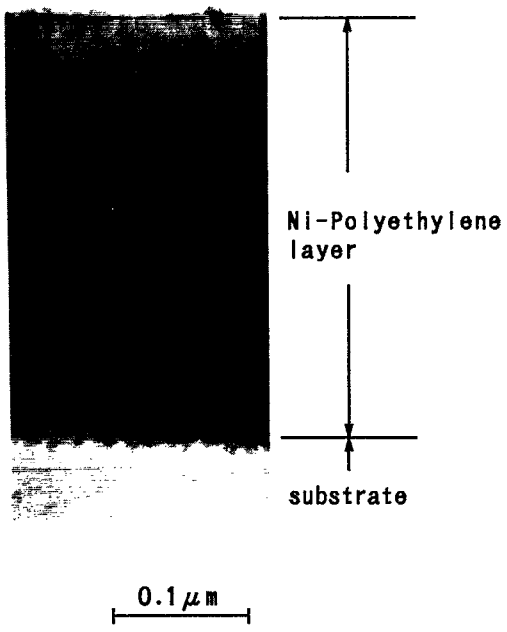

observed peaks are attributed to polycrystalline Ni. The peaks observed before the heat treatment are broader and weaker than those observed thereafter. This indicates that the Ni crystallites before the heat treatment are very small and that these crystallites grow via the treatment. Figure 8 shows a cross-sectional TEM view of a Ni-PE film prepared under the same deposition conditions as sample h. The film has a columnar structure with each column consisting of many micrograins of 100–200 Å.

In Sec. III A it was suggested that the Ni-PE films contain a large amount of the nonmagnetic or very weak ferromagnetic substance. No peaks attributed to such a substance were observed in the x-ray diffraction patterns. It is therefore considered that the Ni-PE films consist of microcrystalline Ni and much smaller microcrystalline or amorphous Ni compounds with very weak or no magnetism.

C. Internal stress

Figure 9 shows the M_s dependence of the internal stress of Ni-PE films (samples i–o). The Ni-PE films have tensile internal stresses as large as $1\text{–}3\times10^{10}$ dyn/cm^2. The values are 10–100 times larger than those of Ni films prepared by triode and diode sputtering methods.[9] This result suggests the possibility that the inverse magnetostrictive effect contributes to the large perpendicular anisotropy of the Ni-PE coevaporated films.

IV. DISCUSSION

The relationship between the $K_{u_\perp}$ and M_s^2 in Fig. 6 suggests that the origin of the perpendicular anisotropy of the Ni-PE films is related to shape anisotropy. The existence of large tensile internal stress in the films suggests that

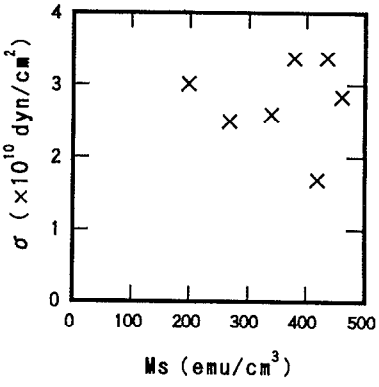

FIG. 9. Saturation magnetization M_s dependence of the internal stress (σ) in the Ni-PE films (samples i–o) listed in Table II.

the induced anisotropy by the inverse magnetostrictive effect also contributes to the perpendicular anisotropy.

In this section we discuss the origin of the perpendicular magnetic anisotropy of the Ni-PE coevaporated films.

A. Shape anisotropy

The existence of the columnar structure shown in Fig. 8 suggests that the shape anisotropy due to this structure contributes to the perpendicular anisotropy of the Ni-PE films. To examine this possibility, we calculated the shape anisotropy based on the simplified model shown in Fig. 10, where Ni prisms are separated from each other by a nonmagnetic substance. The shape anisotropy energy for this configuration was derived by Iwata, Prosen, and Gran[10] as follows:

$$K_{\perp\,\mathrm{calc}}=2\pi M_{s_{\mathrm{Ni}}}^2\left\{\frac{1}{2}\left(\frac{D}{D+d}\right)^2\left[3\left(\frac{D}{D+d}\right)-1\right]+\frac{3D^2}{\pi^3L(D+d)}\sum_{m=1}^{\infty}\frac{1}{m^3}\sin^2\frac{m\pi D}{D+d}\times\left[1-\exp\left(-\frac{2m\pi L}{D+d}\right)\right]+\frac{3(D+d)}{\pi^5L}\times\sum_{m=1}^{\infty}\sum_{n=1}^{\infty}\frac{1}{m^2n^2(m^2+n^2)^{1/2}}\sin^2\frac{m\pi D}{D+d}\times\sin^2\frac{n\pi D}{D+d}\left[1-\exp\left(-\frac{2\pi(m^2+n^2)^{1/2}L}{D+d}\right)\right]\right\},\tag{1}$$

where $M_{s_{\mathrm{Ni}}}$ is the saturation magnetization of the prisms (bulk Ni), L is the height of the prisms (film thickness), D the length of the prism side, and d the gap between the prisms. From the cross-sectional TEM view in Fig. 8, L and $D+d$ were set to 5000 and 100 Å, respectively. The quantity d/D is determined by Eq. (2) which expresses that the ratio of the saturation magnetization of the film to that of bulk Ni is equal to the volumeric packing ratio of the Ni prisms in the film,

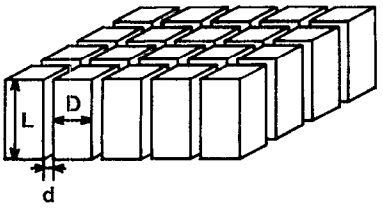

FIG. 10. Columnar structure model for calculating the shape anisotropy. The prisms are infinitely distributed in a grid pattern. The dimensions of any prism are $D\times D\times L$. The gap length between the prisms is d (Ref. 10).

$$M_{s_{\text{Ni-PE}}}/M_{s_{\text{Ni}}}=V_{\text{Ni}}/V=D^2/(D+d)^2, \tag{2}$$

where $M_{S_{\text{Ni-PE}}}$ and $M_{S_{\text{Ni}}}$ are the saturation magnetizations of the Ni-PE films and bulk Ni, respectively, V the total volume of the film, and V_{Ni} the volume of the Ni prisms. Figure 11 shows the M_s dependence of the calculated shape anisotropy energy ($K_{\perp\ \text{calc}}$) along with experimental data on the Ni-PE films. $K_{\perp\ \text{calc}}$ is positive in the range of 0–160 emu/cm^3. In the whole saturation magnetization range, the $K_\perp$ is much larger than $K_{\perp\ \text{calc}}$. Consequently, the contribution of the shape anisotropy to the perpendicular anisotropy of the Ni-PE films appears to be very small.

B. Magnetocrystalline anisotropy

A very weak preferential orientation of Ni(111) parallel to the substrate was observed in the x-ray diffraction pattern [Fig. 7(a)]. It is necessary to take into account the magnetocrystalline anisotropy of the Ni crystal since the axis of easy magnetization lies in the ⟨111⟩ axis. The magnetocrystalline anisotropy energy K_{crys} averaged around the principal axis (Ni⟨111⟩) is expressed as

$$K_{\text{crys}}=K_1(\tfrac{7}{12}\sin^4\theta-\tfrac{2}{3}\sin^2\theta)$$
$$+K_2(-\tfrac{1}{7}\sin^6\theta+\tfrac{5}{12}\sin^4\theta-\tfrac{2}{9}\sin^2\theta), \tag{3}$$
$$K_1=-5.7\times10^4\ \text{erg/cm}^3,$$
$$K_2=-2.3\times10^4\ \text{erg/cm}^3,$$

where K_1, K_2 are the magnetocrystalline anisotropy constants of bulk Ni,[11] and θ is the angle between the magnetic moment vector and Ni⟨111⟩. A full derivation of Eq. (3) is given in the Appendix. Assuming that the Ni-PE films consist of Ni crystallites and the nonmagnetic substance, the magnetocrystalline anisotropy energy of the Ni-PE films ($K_{\text{crys}_{\text{Ni-PE}}}$) can be expressed as follows:

$$K_{\text{crys}_{\text{Ni-PE}}}=(V_{\text{Ni}}/V)K_{\text{crys}}=(M_{s_{\text{Ni-PE}}}/M_{s_{\text{Ni}}})K_{\text{crys}}, \tag{4}$$

where V_{Ni} is the volume of Ni crystallites and V the total volume of the film. If Ni⟨111⟩ perfectly orients to the normal direction of the film, $K_{\text{crys}_{\text{Ni-PE}}}$ is obtained by substituting K_{crys} in Eq. (3) into Eq. (4). The difference of K_{crys} between the maximum and minimum value is calculated to be 1.1×10^4 erg/cm^3. Taking into account the facts that $M_{s_{\text{Ni-PE}}}/M_{s_{\text{Ni}}}\leqslant 1$ and that the orientation of Ni⟨111⟩ to the film normal is not good, $K_{\text{crys}_{\text{Ni-PE}}}$ is far smaller than the observed perpendicular anisotropy energy (0.5–1×10^{-6} erg/cm^3) of the Ni-PE films. The magnetocrystalline anisotropy of Ni scarcely contributes to the perpendicular anisotropy of the Ni-PE films.

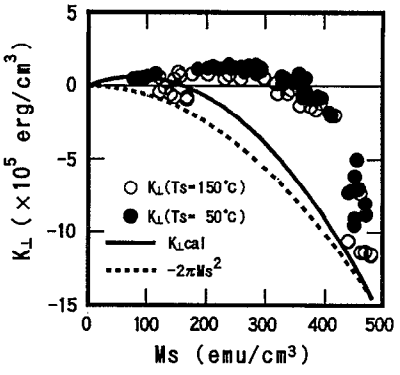

FIG. 11. Saturation magnetization M_s dependence of the induced anisotropy energy ($K_{s_{\text{calc}}}$) calculated by Eqs. (1) and (2) and $-2\pi M_s^2$. Experimental data on the perpendicular anisotropy energy $K_\perp$ (○, ●) are also plotted.

C. Induced anisotropy by inverse magnetostrictive effect

Magnetic anisotropy can be induced in the film by an internal stress through the inverse magnetostrictive effect. The anisotropy energy K_s induced by the inverse magnetostrictive effect is given by the following equation for the assembly of randomly oriented particles:

$$K_s=\tfrac{3}{2}\lambda\sigma, \tag{5}$$

where λ is the magnetostriction constant and σ the stress. Assuming that the Ni-PE films are composed of Ni crystallites and the nonmagnetic substance, perpendicular anisotropy can be induced in the Ni-PE films through the inverse magnetostrictive effect since these films have large tensile internal stress (Fig. 9) and the magnetostrictive constants λ_{111} and λ_{100} of bulk Ni are negative.[12] The induced magnetic anisotropy of the Ni-PE films $K_{s_{\text{Ni-PE}}}$ by the inverse magnetostrictive effect is calculated by the following equation:

$$K_{s_{\text{Ni-PE}}}=(M_{s_{\text{Ni-PE}}}/M_{s_{\text{Ni}}})K_s. \tag{6}$$

To calculate the energy, data on the internal stress in Fig. 9 and the magnetostrictive constant of isotropic polycrystalline Ni(32.9×10^{-6}) (Ref. 12) are adapted. The $K_{s_{\text{Ni-PE}}}$ and $K_{u_\perp}$ of the Ni-PE films are plotted against M_s in Fig. 12. The M_s dependence of the $K_{s_{\text{Ni-PE}}}$ is coincident with that of the $K_{u_\perp}$ except for the higher M_s region above 400 emu/cm^3. The reason for the difference between the $K_{s_{\text{Ni-PE}}}$ and $K_{u_\perp}$ in this region is now being investigated.

Corner and Hunt[13] measured the temperature dependence of the magnetostriction constants λ_{111} and λ_{100} of bulk Ni, and found that these constants are proportional to the square of the saturation magnetization. Assuming that

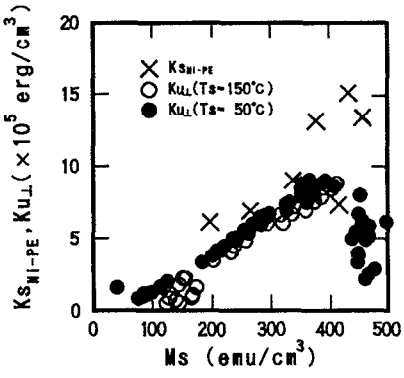

FIG. 12. Saturation magnetization M_s dependence of the induced anisotropy energy ($K_{s_{Ni\text{-}PE}}$) (×) by the inverse magnetostrictive effect and the intrinsic perpendicular magnetic anisotropy energy ($K_{u_\perp}$) (○, ●).

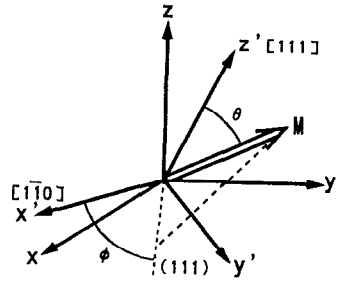

FIG. 13. Coordinate systems. The x, y, and z axes in the $S(x,y,z)$ coordinate system are taken along with the principal axes of a cubic crystal. The x'-y' plane in the $S'(x',y',z')$ coordinate system is taken on the (111) plane and the x' and z' axes are taken along with the [110] and [111] axes, respectively. The magnetization vector has an inclination angle θ and an azimuthal angle ϕ in the S' coordinate system.

the internal stress of the Ni-PE films is constant in the temperature range of −195–150 °C, the temperature dependence of the $K_{s_{Ni\text{-}PE}}$ is as follows:

$$K_{s_{Ni\text{-}PE}} \propto \lambda\sigma \propto M^2_{s_{Ni\text{-}PE}}. \tag{7}$$

The relation between the $K_{u_\perp}$ and M_s^2 (bold lines in Fig. 6) in the temperature range of −195–150 °C can be explained by Eq. (7).

Conclusively, it is considered that the uniaxial induced magnetic anisotropy by the inverse magnetostrictive effect plays an important role in originating the perpendicular anisotropy of the Ni-PE films.

V. CONCLUSIONS

To investigate the origin of perpendicular anisotropy of the Ni-PE films, the temperature dependence of the magnetic properties (M_s, $H_{c_\perp}$, and $K_\perp$), the crystallographic structures and the internal stress were measured. Our experimental results and considerations on the origin of the anisotropy allow us to draw the following conclusions.

(i) The saturation magnetization at room temperature of Ni-PE films rapidly decreases as the carbon content increases. The magnetic properties change irreversibly by the heat treatment up to 425 °C. In x-ray diffraction measurement of the Ni-PE films, all observed peaks before and after the heat treatment can be attributed to polycrystalline Ni. The peaks observed before the treatment are broader and weaker than those observed thereafter. According to the results, it is considered that the Ni-PE films are composed of microcrystalline Ni and microcrystalline or amorphous Ni compounds whose magnetism is very weak or nonexistent.

(ii) The Ni-PE films have tensile internal stresses as large as $1\text{–}3\times10^{10}$ dyn/cm^2.

(iii) According to the data on the dependence of the perpendicular magnetic anisotropy of the Ni-PE films on saturation magnetization and temperature, the anisotropy is considered to be induced by the internal stress in the films through the inverse magnetostrictive effect.

APPENDIX

Let us take the two orthogonal coordinate systems of $S(x,y,z)$ and $S'(x',y',z')$ as shown in Fig. 13. The x, y, and z axes in the S coordinate system are taken along with the principal axes of a cubic crystal. The x'-y' plane in the S' coordinate system is on the (111) plane, and the x' and z' axes are taken along with the [1$\bar{1}$0] and [111] axes, respectively. The relationship between the two sets of the direction cosines of these coordinate systems is given as follows:

$$\begin{pmatrix}\alpha_1\\ \alpha_2\\ \alpha_3\end{pmatrix} = \begin{pmatrix} \frac{1}{\sqrt{2}} & \frac{1}{\sqrt{6}} & \frac{1}{\sqrt{3}} \\ -\frac{1}{\sqrt{2}} & \frac{1}{\sqrt{6}} & \frac{1}{\sqrt{3}} \\ 0 & -\frac{\sqrt{2}}{\sqrt{3}} & \frac{1}{\sqrt{3}} \end{pmatrix} \begin{pmatrix}\alpha'_1\\ \alpha'_2\\ \alpha'_3\end{pmatrix}, \tag{A1}$$

where $(\alpha_1,\alpha_2,\alpha_3)$ and $(\alpha'_1,\alpha'_2,\alpha'_3)$ are the sets of the direction cosines of the S and S' coordinate systems, respectively. When the magnetization vector $\mathbf{M}$ has an inclination angle θ, an azimuthal angle ϕ in the S' coordinate system and a set of the direction cosines $(\alpha'_1,\alpha'_2,\alpha'_3)$ with respect to the S' coordinate system, these direction cosines are expressed as follows:

$$\alpha'_1=\sin\theta\cos\phi, \quad \alpha'_2=\sin\theta\sin\phi, \quad \alpha'_3=\cos\theta. \tag{A2}$$

The magnetocrystalline anisotropy K for cubic crystal is given in terms of the direction cosines $(\alpha_1,\alpha_2,\alpha_3)$ with respect to the S coordinate system as

$$K=K_1(\alpha_1^2\alpha_2^2+\alpha_2^2\alpha_3^2+\alpha_3^2\alpha_1^2)+K_2\alpha_1^2\alpha_2^2\alpha_3^2+\cdots, \tag{A3}$$

where K_1 and K_2 are the magnetocrystalline constants.

Substituting the two relations [Eqs. (A1) and (A2)] into Eq. (A3), and averaging the energy K over the range of ϕ from 0 to 2π, we obtain the following equation [Eq. (3) of the main text]:

$$K_{crys}=K_1(\tfrac{7}{12}\sin^4\theta-\tfrac{2}{3}\sin^2\theta) + K_2(-\tfrac{1}{7}\sin^6\theta+\tfrac{5}{12}\sin^4\theta-\tfrac{2}{9}\sin^2\theta).$$

[1] J. Perrin, B. Despax, and E. Kay, Phys. Rev. B **32**, 719 (1985).
[2] C. Laurent and E. Kay, J. Appl. Phys. **65**, 1717 (1989).
[3] N. Boonthanom and M. White, Thin Solid Films **24**, 295 (1974).
[4] C. Laurent, D. Mauri, E. Kay, and S. S. P. Parkin, J. Appl. Phys. **65**, 2017 (1989).
[5] T. Maro, O. Kitakami, and H. Fujiwara, Jpn. J. Appl. Phys. **27**, L687 (1989).
[6] T. Maro, O. Kitakami, and H. Fujiwara, Jpn. J. Appl. Phys. **29**, 860 (1990).
[7] T. Maro, O. Kitakami, and H. Fujiwara, J. Magn. Soc. Jpn. **13**, Suppl. S-1, 369 (1989).
[8] P. Weiss and R. Forrer, Compte Rend. **178**, 1670 (1924).
[9] K. Sato, H. Kondo, and T. Mizoguchi, J. Appl. Phys. **64**, 5440 (1988).
[10] T. Iwata, R. J. Prosen, and B. E. Gran, J. Appl. Phys. **37**, 1285 (1966).
[11] J. J. M. Franse and G. de Vries, Physica **39**, 477 (1968).
[12] E. W. Lee, Rep. Prog. Phys. **18**, 184 (1955).
[13] W. D. Corner and G. H. Hunt, Proc. Phys. Soc. A **68**, 133 (1955).